

**Early stage reactivity and in-vitro behavior of silica-based bioactive glasses  
and glass-ceramics.**

E. Verné\* , O. Bretcanu\* , C. Balagna\* , C. L. Bianchi# , M. Cannas^ , S. Gatti^ , C. Vitale-  
Brovarone\*

This is the author post-print version of an article published on  
*Journal of Materials Science: Materials in Medicine*, Vol. 20, pp.  
75-87, 2009 (ISSN 0957-4530).

The final publication is available at [link.springer.com](http://link.springer.com).

This version does not contain journal formatting and may contain  
minor changes with respect to the published edition.

The present version is accessible on PORTO, the Open Access  
Repository of the Politecnico of Torino, in compliance with the  
publisher's copyright policy.

Copyright owner: *Springer*.

\* Materials Science and Chemical Engineering Department, Politecnico di Torino, C.so  
Duca degli Abruzzi 24, 10129 Torino, Italy

# Physical Chemistry & Electrochemistry Department, Università di Milano, Via Golgi  
19, 20133 Milano, Italy

^ Department of Medical Sciences, Human Anatomy, University of Eastern Piedmont,  
Via Solaroli 17, 28100 Novara, Italy

## **Abstract**

The surface reactivity of different sets of glasses and glass-ceramics belonging to the  $\text{SiO}_2\text{-P}_2\text{O}_5\text{-CaO-MgO-K}_2\text{O-Na}_2\text{O}$  system have been investigated. The attention was focused on the role of their composition on the bioactivity kinetics, in terms of pH modifications, silica-gel formation and its evolution toward hydroxycarbonatoapatite, after different times of soaking in simulated body fluid. Glasses and glass ceramics have been characterized by thermal analysis, SEM-EDS observations and phase analysis (XRD). XPS measurements have been carried out on the most representative set of sample in order to evaluate the evolution of the surface species during the growth of silica-gel and hydroxycarbonatoapatite. The response of murine fibroblast 3T3 to the material before and after a conditioning pre-treatment (immersion in SBF) has been investigated on the same set of samples in order to point out the role of the bioactivity mechanism on cell viability. The main differences among the various glasses have been related to the modifier oxides ratio and to the MgO content, which seems to have an influence on the glass stability, both in terms of thermal properties and surface reactivity. The surface characterization and in vitro tests revealed few variations in the reactivity of the different glasses and glass-ceramics in their pristine form. On the contrary, the different surface properties before and after the pre-treatment in SBF seem to play a role on the biocompatibility of both glass and glass-ceramics, due to the different ion release and hydrophilicity of the surfaces, affecting both cell viability and protein adsorption.

## 1 Introduction

Bioactive glasses and glass-ceramics represent a class of attractive materials for use in bone reconstruction [1]. Their surface reactivity on contact with biological fluids is widely studied [2, 3]. The growing interest in these systems is based on their ability to induce *in vitro*, by immersion in a simulated body fluid (SBF), the formation of a semi-crystalline hydroxycarbonatoapatite (HCA) rich layer. This behavior is considered as an indication of their *in vivo* bioactivity (natural bonding ability to living tissues) through a mechanism that involves the formation of a biological-like HCA layer onto the material surface [4-6]. As reported in the literature, the bioactivity mechanism starts with a rapid ions exchange between the alkaline ions from the glass surface and the hydrogen ions from the solution, followed by the formation of silanols, which then undergo polycondensation to develop a silica gel layer. This layer promotes the adsorption of  $\text{Ca}^{++}$  and  $\text{PO}_4^{3-}$  ions from the solution. These ions subsequently react, forming the HCA layer. This mechanism, frequently reported in literature, was observed in MgO-containing glasses as well as in MgO-free glasses [7,8]. Some authors reported a decreased ability of apatite formation in glass-ceramic with a higher MgO content [8]. The controversial topic of the influence of the MgO content on the bioactivity properties of glasses and glass-ceramic was recently studied by Oliveira et al. in relation to the  $\text{SiO}_2$  and MgO content [9]. In that work the authors discussed about the role of MgO on the surface reactivity of glasses belonging to the  $\text{SiO}_2\text{-P}_2\text{O}_5\text{-CaO-MgO}$  system, reporting an increasing surface activity with increasing MgO/CaO ratio, since MgO in the glass indirectly improves the early stages of mineralisation by favouring  $\text{SiO}_4^{4-}$  speciation. Previous investigations on the *in vitro* bioactivity of glasses and glass-ceramics containing MgO [10] highlight the influence of both chemical and morphological factors on the surface reactivity.

It is also well known that the first stages of bioactivity, including the formation of silanols on the glass surface, give rise to a depletion of the hydrogen ions in the solution which produces a slight enhancement of pH values. This feature can be also observed in solutions such as TRIS buffer or Kokubo's SBF [9] and should be carefully controlled when bioactive glass samples are placed in contact with different cell lines, during

biological evaluations [11]. The sodium-proton exchange, beside producing a pH variation, could also affect the K/Na ratio in the extracellular matrix, causing unknown effects on cell viability.

For the above mentioned reasons, in the present study different sets of glasses and glass-ceramics belonging to the  $\text{SiO}_2\text{-P}_2\text{O}_5\text{-CaO-MgO-K}_2\text{O-Na}_2\text{O}$  system have been prepared and characterized in terms of thermal properties, devitrification ability and phase analysis. The *in-vitro* surface reactivity of the different sets of glasses and glass-ceramics have been investigated, focusing the attention on the role of their composition on the bioactivity kinetics, as well as on the response of murine fibroblast 3T3 to these material. Cell studies were conducted on the most representative set of samples both before and after a conditioning pre-treatment (immersion in SBF).

## 2 Experimental

### 2.1 Materials synthesis and characterization

Different glasses, belonging to the system  $\text{SiO}_2\text{-P}_2\text{O}_5\text{-CaO-MgO-K}_2\text{O-Na}_2\text{O}$ , were prepared by traditional melt and quenching route. The chosen glasses compositions (mol % of the oxides) are reported in Table I. In order to induce fast surface reaction kinetic, the total amount of glass network former oxides ( $\text{SiO}_2 + \text{P}_2\text{O}_5$ ) was maintained between 45 and 50 % mol.

Some authors reported that glasses with low amounts of silica (below 53% mol) induce a rapid formation of HCA crystals on their surface during soaking in SBF [2]. For the glasses investigated in this study, the silica content ranged from 47.5 to 42.5 mol %. As reported in Table I, this quantity was modified, starting from glasses 47.5A and 47.5B, by increasing the amount of  $\text{P}_2\text{O}_5$  (45A and 45B) or by increasing the total modifier oxides content (42.5A and 42.5B). This allowed the production of glasses progressively more reactive toward aqueous solutions. Moreover, the ratio of the different modifier oxides was tailored in order to investigate the possible role of each oxide (if different one from each other) on the surface reactivity.

The raw materials ( $\text{SiO}_2$ ,  $\text{Ca}_3(\text{PO}_4)_2$ ,  $\text{CaCO}_3$ ,  $\text{K}_2\text{CO}_3$ ,  $\text{Na}_2\text{CO}_3$ ) were intimately mixed and heated, in a platinum crucible, up to  $1500^\circ\text{C}$  at a scan of  $500^\circ\text{C}/\text{hour}$ . The melt was maintained at  $1500^\circ\text{C}$  for 3 hour and than poured on a brass plate, obtaining bars, or quenched in cold water, obtaining a frit. After quenching, the frit was dried, than ground by ball milling and sieved to a final grain size below  $40\mu\text{m}$ . The glass transition ( $T_g$ ) and crystallization ( $T_x$ ) temperatures were determined on powders by means of a differential thermal analysis (DTA7 Perkins Elmer).

The poured amorphous bars were annealed, or thermally treated in order to produce glass-ceramic specimens. The annealing and devitrification conditions were deduced from the characteristic temperatures previously detected by DTA. After annealing or devitrification, glass and glass-ceramic bars were cut in slices of 1 mm thickness and about 1 square cm area, using a diamond blade.

The nature and morphology of the crystalline phases in the glass-ceramic samples were investigated through X-Ray diffraction (XRD) and scanning electron microscopy (SEM) equipped with energy dispersive spectrometer (EDS). For the morphological and compositional studies, glass-ceramic slices were chemically etched for 30 seconds with a 5% mol.  $\text{HF}/\text{HNO}_3$  (1:1) solution to remove the amorphous phase.

## 2.2 *In vitro* bioactivity

The *in vitro* bioactivity was investigated observing the formation of silica gel and hydroxycarbonatoapatite (HCA) on the surface of each glass and glass-ceramic, after different times of soaking in simulated body fluid (SBF). Slices of each glass and glass-ceramic were soaked in SBF (prepared following Kokubo's protocol) [12] for different periods of time, up to 56 days. Specifically, the slices were soaked in 25 ml of SBF in polyethylene bottles with or without refreshing the solution. In a set of samples the solution was changed every 48 hours to simulate the recirculation of physiological fluids. To evaluate the formation of a silica gel layer and of hydroxycarbonatoapatite (HCA) aggregates on the glass surface, slices were characterised, after different soaking periods, by X-ray diffraction (X'Pert Philips diffractometer) using the Bragg Brentano camera geometry and the  $\text{CuK}\alpha$  incident radiation. Scanning electron microscopy (SEM Philips

525M) with compositional analyses (EDS, Philips-EDAX 9100) were used to evaluate the amount and morphology of the precipitated HA on the surface of the soaked slices.

During soaking in SBF, pH evaluations were performed on each solution, to monitor the pH variations due to ion exchange processes between bioactive glasses or glass-ceramics and the surrounding fluids. All the in vitro bioactivity experiments were carried out in triplicate.

On the most representative sample (47.5A glass) X-ray photoelectron (XPS) measurements, after different times of soaking in SBF, were carried out. XPS spectra were taken in an M-probe apparatus (Surface Science Instruments). The source was monochromatic AlK $\alpha$  radiation (1486.6 eV). A spot size of 400x1000 $\mu$ m and pass energy of 150 eV were used for survey spectra, while for the single-region acquisitions a spot size of 200x750  $\mu$ m and a pass energy of 25 eV were used. Resolutions were 1.39 and 0.74, respectively. The energy scale was calibrated with reference to the 4f<sub>7/2</sub> level of a freshly evaporated gold sample, at 84.0  $\pm$  0.1 eV, and with reference to the 2p<sub>3/2</sub> and 3s levels of copper at 932.5  $\pm$  0.1 and 122.39  $\pm$  0.15 eV, respectively.

The binding energies (BE) were corrected for specimen charging by referencing the C 1s peak to 284.6 eV, and the background was subtracted using Shirley's method.

The peak fitting was performed using only Gaussian line shapes. The accuracy of the reported BE can be estimated to be  $\pm$  0.1 eV. With a monochromatic source, an electron flood gun is required to compensate the build up of positive charge on the samples during the analyses, when insulating samples are analyzed: a value of 10 eV has been selected.

This technique was effective in order to follow the evolution of the chemical species on the glass surface during the various steps of surface modification. In details, after the washing treatments the samples were put inside the instrument without further pretreatments. The following regions were investigated: Si 2p to detect the nature of the silica and its change after the different performed washing processes; O 1s to investigate the presence of structural oxygens and/or OH<sup>-</sup> groups; C1s to evaluate the presence of carbonate species.

### 2.3 *Biological characterization*

Preliminary cytocompatibility tests were performed on the most representative set of samples, before and after soaking for 1 week in SBF. Proteins adsorption, adhesion and proliferation test were performed using murine fibroblast NIH-3T3 cultured in Modified Dulbecco's Medium (DMEM) supplemented with 10% (v/v) fetal bovine serum (FBS, Sigma), 100 U/ml penicillin, 100 µl streptomycin and 0,03% L-glutamine at 37 °C in 95% air/5% CO<sub>2</sub>.

The area of each sample was calculated using Leica Qwin programme. The materials were sterilized in stove at 180 °C for 3h before the cell test. For adhesion (3 hours) were assessed by seeding  $2 \times 10^4$  cells/cm<sup>2</sup> and  $5 \times 10^3$  cells/cm<sup>2</sup>; for proliferation (5 days), cells cultured on polystyrene were used as positive control.

After 3h the materials were washed twice with PBS, then the cells were detached by trypsin, that was neutralized with fresh medium with 10% of FBS. The medium was collected in test tube for analysis using a cytofluorimeter. The spontaneous fluorescence of material doesn't allow the use of other staining normal accepted for the count of cells, like a Acridine Orange. After 2 days the fresh medium was added, and on day five, the cells were counted.

Proteins adsorption assays were performed using human platelets poor plasma obtained by centrifugation at 2000g for 15 min at 4°C of venous blood from four healthy donors, collected in siliconized tubes containing 3.5% (w/v) sodium citrate (Becton Dickinson, Meylan, France). The materials were incubated with 200 µL PPP for 30 min at room temperature; a polystyrene plastic well were used as control. After incubation the samples were washed three times in phosphate-buffer saline (PBS) and the materials were incubated for 4 hours in 200 µL of a solution 1% of sodium dodecyl sulfate (SDS). Adsorbed proteins were measured using a commercial protein quantification kit (Pierce, Rockford, IL) based on bicinchoninic acid (BCA). The optical densities were read at 562 nm, and the results were expressed in micrograms of protein per millilitre.

Samples were loaded onto a separating polyacrylamide gel. Proteins were blotted onto nitrocellulose membrane (Amersham, Milan, Italy) in a BioRad Mini Trans-Blot Electrophoretic Transfer Cell. The membranes were incubated with rabbit anti-human

IgG, IgA, (Dako, Milan, Italy) 5 mg/mL in PBS overnight at 4°C, and then with a secondary antibody conjugated with horseradish peroxidase (Amersham). ECL Western blotting detection reagents (Amersham) were used for immunodetection of the eluted proteins.

### **3 Results and Discussion**

#### *3.1 Thermal and phase characterization of the virgin glasses and glass-ceramics*

Two of the six glasses reported in this study (45A and 42.5B) underwent a rapid devitrification during cooling from the melting temperature of their precursors to room temperature. The only common feature of these glasses is the low Na<sub>2</sub>O/K<sub>2</sub>O ratio. K<sub>2</sub>O is known as a good nucleating agent, so this could reasonably explain the easiness of devitrification in those two systems. For this reason 45A and 42.5B were not characterized, since one of the objectives of this work was the comparison between glasses and glass-ceramics of the same parent system.

The thermal characterization performed on the other four glasses (Table II) gave information on the proper annealing temperature and on the crystallization treatment. The DTA thermal scans of three of the investigated glasses (47.5A, 42.5A and 45B samples) show two different exothermic peaks (corresponding to the crystallization peaks of two different crystalline phases) and two different endothermic peaks (corresponding to the melting process of each of these two phases).

Very few differences have been detected among the characteristic temperatures of the various glasses. XRD analysis on glass-ceramics show a typical pattern with some crystalline phases, identified as a mixture of sodium/calcium silicates and potassium/calcium silicates. For example, the XRD patterns of 47.5A glass and the corresponding glass-ceramic are reported in figure 1. The pattern of the glass shows the typical broad peak between 25° and 45°, while the pattern of the glass-ceramic shows the characteristic peaks of Na<sub>2</sub>CaSi<sub>3</sub>O<sub>8</sub> (JCPDF file n. 00-012-0671) and K<sub>4</sub>Ca[SiO<sub>3</sub>]<sub>3</sub> (JCPDF file n. 00-039-1427) crystals, and an amorphous halo at lower angles. SEM

observations on the chemically etched surface of the 47,5A glass-ceramic sample revealed two different crystal morphologies (fig. 2): needle-like shaped crystals, probably  $\text{Na}_2\text{CaSi}_3\text{O}_8$ , and cubic crystals, probably  $\text{K}_4\text{Ca}[\text{SiO}_3]_3$ , which crystallizes in the cubic system.

Considering the characteristic temperatures of the two glasses 47.5A and 47.5B, it can be observed that the second crystallization peak in the 47.5B sample is absent, and that 47.5A, which contains MgO oxide, has a lower Tg. (Table II). The XRD pattern of the 47.5B glass-ceramic confirms the first result, since it is characterized by the presence of only one phase ( $\text{Na}_2\text{CaSi}_3\text{O}_8$ ). The 47.5B glass contains 10 mol % MgO which is absent in the 47.5A. The addition of 10% mol MgO in the glass composition can explain the difference in the crystallization process of the two glasses. The presence of this oxide in the glass can produce a broadening of the range between the glass transition point (Tg) and the crystallization point [13]. This feature could be related to a higher stability of the  $\text{Mg}^{2+}$  containing glass, which in turn could be related with the inhibition of the crystallization of one phases (probably the less stable  $\text{K}_4\text{Ca}[\text{SiO}_3]_3$ ). On the other hand, the lower content of CaO, partially substituted by MgO, can simply explain the formation of only one silicate ( $\text{Na}_2\text{CaSi}_3\text{O}_8$ ), which is the more stable of the two.

Considering the characteristic temperatures of 42,5A and 45B glasses, it can be observed that the 42,5A glass shows characteristic temperatures at higher values if compared with 45B, especially the value of the first crystallization peak. Also in this case is evident a broadening of the range between the glass transition point and the crystallization point. Again, the increased thermal stability can be related to the higher content of MgO. Both 42,5A and 45B glasses, when submitted to a thermal treatment, produces the nucleation and growth of various mixed silicates, containing Na, Ca and Mg in different amounts.

### *3.2 In vitro bioactivity of 47.5A, 42.5A, 47.5B and 45B systems*

On the four systems previously characterized, the *in vitro* bioactivity have been investigated, with the aim of observing in a preliminary step their behavior in contact with a simulated body fluid.

### 3.2.1 pH analysis

Figures 3.a-d show the pH variations detected during soaking in SBF, without refresh of the solution, of all glasses and their corresponding glass-ceramics. The higher value after 20 days (9.21) was observed with the glass 47.5A. The glass 42.5A also produces a high pH value, due to the large amount of modifiers oxides in its composition. The glass 47.5B gives lower pH values when compared with the glass 47.5A, probably due to the presence of MgO. In fact,  $Mg^{++}$  ions can form complexes with the  $OH^-$  ions present in the solution, which could give rise to a weak buffering effect [14].

The glass 45B shows intermediate pH values, between those of 47.5A and 47.5B. This feature could be related to the intermediate amount of MgO amount (5 mol %) in its composition, when compared with 47.5B (10 mol %) and 47.5A (0 mol %) glasses.

During the first two weeks, the pH values of the solutions in contact with glasses were slightly higher than those of the solutions in contact with glass-ceramics. This phenomenon is explained by considering that the amorphous phase is usually more prone to ion leaching phenomena than crystalline phases. The effect on the solution pH is related to this ion leaching.

### 3.2.2. Phase analysis (XRD)

The XRD analyses performed on the different samples after soaking in SBF revealed the evolution of the pattern towards HCA in about 14 days, which became more defined at 21 days on each glass and glass-ceramic sample, with few differences in the definition of the pattern. The glass-ceramic samples were generally less reactive than their parent glass. However, the 47,5A and 47,5B glass ceramics displayed a higher reactivity when compared with the other two glass-ceramics, probably due to the presence of a slightly larger quantity of the residual amorphous phase, revealed by a more evident broad halo. For both 47,5A and 47,5B glass ceramics the broad halo, attributed to the residual amorphous phase, disappears after soaking in SBF, due to the growth of HCA on top of their surfaces and to the partial dissolution of the amorphous phase. The amorphous phase the main phase involved in the ion leaching mechanism during early stages of

bioactivity. In the case of 45B and 42,5A glass-ceramics, the peaks corresponding to HCA after 14 days of immersion are less well defined in respect to their parent glasses.

### *3.2.3 Morphology and composition (SEM-EDS)*

SEM observation and EDS analyses performed on each sample after different times of soaking in SBF confirmed these data, since well defined globular agglomerates of HCA on the top of a silica gel layer have been detected after 21 days, especially on 47,5A. As an example SEM micrographs of the four glass system after 21 days of soaking are reported in figure 4.a –d.

### *3.3 In vitro bioactivity of 47,5A: detailed analysis*

As the differences in the pH values obtained after soaking in SBF for most of the glasses and glass ceramics are small, further studies have been focused on the most reactive samples: 47,5A glass and glass-ceramic. Therefore, a more detailed investigation of the bioactivity in SBF was performed only on 47,5A glass and glass-ceramic, which seemed to be slightly more reactive than the other investigated systems. Thus, a set of 47,5A samples was soaked in SBF for longer periods of time (7, 28 and 56 days) in order to asses their reactivity. Another set of samples was soaked in SBF for 3, 7, 10, 15 days with the solution being changed every 48 hours. The refreshing of the solution is an easy way to simulate the *in vivo* conditions. In this way a more accurate evaluation of the samples reactivity in the early stages of immersion in SBF was possible.

#### *3.3.1 pH analysis*

The pH value was monitored for both sets of samples during soaking. For the set of samples where the refresh was performed, the pH never exceeded the value of 8, while in the case of the samples in which the solution was not refreshed the trend was towards higher pH values.

### 3.3.2 Phase analysis (XRD)

In the case of the 47.5A glass soaked without refresh (figure 5.a), after 7 days of soaking a broad amorphous halo was detected at small diffraction angles (between  $20^\circ$  and  $30^\circ$ ). This halo can be attributed to the developing of a gel-like phase (typically, the silica-gel produced during the first stages of bioactivity). The precipitation of HCA was observed after 28 days of soaking and is gradually developed up to 56 days. If the solution is refreshed (figure 5. b) the formation of both silica-gel and HCA is faster. In fact, the broad halo between  $20^\circ$  and  $30^\circ$  is observed after only 3 days of immersion and the precipitation of HCA starts after 10 days, showing well defined crystals after 15 days.

In the case of the 47.5A glass-ceramic (figure 6.a and 6.b), beside the signals of HCA, the peaks corresponding to  $\text{Na}_2\text{CaSi}_3\text{O}_8$  are still present, while the peaks corresponding to  $\text{K}_4\text{Ca}[\text{SiO}_3]_3$  disappeared after few days of immersion (probably due to its higher solubility).

The presence of  $\text{Na}_2\text{CaSi}_3\text{O}_8$  seems to slightly enhance the glass-ceramic bioactivity (which is faster in comparison to the completely amorphous 47.5A). The HCA formation might be faster in the glass-ceramic due to the nucleating effect of the crystalline phase. Moreover, the refreshing of the solution increases the kinetics of the surface reactions.

### 3.3.3. Morphology and composition (SEM-EDS)

XRD results were confirmed by SEM-EDS analysis (figures 7-10). The surface morphology and EDS analysis on the 47.5A glass after 7 (a), 28 (b) and 56 (c) days of immersion in SBF without refreshing the solution are reported in figure 7. It can be seen that after 7 days of soaking, the gel-like layer formed on the sample surfaces contains Si, Ca and P. With increasing the soaking time up to 56 days, this layer became more rich in Ca and P and less rich in Si, and transformed into well defined formation of agglomerates, typical of microcrystalline HCA.

Figure 8 reports the SEM images and EDS analysis on the glass 47.5A after 3 (a), 7 (b), 10 (c) and 15 (d) days of immersion in SBF with refresh of the solution. In this case, after three and seven days of soaking in SBF the gel-like layer, rich in Ca and P, is

progressively less rich in Si, and the precipitation of globular HCA is apparent after 10 days. The morphology of this layer after 15 days in SBF (figure 8.d) shows that the HCA agglomerates are well embedded into the gel-like layer. The HCA crystals were probably formed by incorporation of  $\text{Ca}^{++}$  and  $\text{PO}_4^{3-}$  ions into the gel-like layer, according to the Hench mechanism [2].

Figure 9 and 10 reports the results of SEM-EDS analysis performed on the 47,5A glass-ceramic, after soaking in SBF with and without refreshing the solution. In the case of the samples soaked without refreshing the solution (figure 9), the nucleation of HCA is faster when compared with that of the the parent glass, probably due to the nucleating effect of the crystalline phase. As can be seen in figure 9.a, different globular agglomerates are visible on the gel-like layer after 7 days of immersion in SBF. EDS analysis shows a higher enrichment in Ca and P of this layer, in comparison to the glass after the same period of immersion (figure 7.a). This result is in perfect agreement with the XRD analysis reported in figure 6, where after 7 days of immersion both the broad halo of the amorphous gel-like layer and the main peaks of HCA are present. The precipitation of globular agglomerates of HCA is gradually more evident during soaking up to 56 days, as reported in figures 9.b and 9.c.

For the glass-ceramic samples soaked in SBF with refreshing of the solution, both the gel-like film rich Ca and P and some small agglomerates of HCA are observed after after 3 days (figure 10.a –d). This layer evolves toward a more structured one within 15 days. The SEM-EDS observation, in conjunction with the XRD analyses are in agreement with the well known bioactivity mechanism [2], which involves after surface leaching with sodium-proton exchange and loss of soluble silica, the formation of a hydrated silica gel-like film by polycondensation of silanols, development of an amorphous calcium-phosphate layer onto or into the silica-rich layer by incorporation od  $\text{Ca}^{++}$  and  $\text{PO}_4^{3-}$  ions, and its crystallization as hydroxycarbonatoapatite.

#### *3.3.4 X-ray photoelectron spectroscopy*

The evolution of the surface of 47,5A glass was monitored by XPS measurements, following the procedure above described.

XPS spectra of the Si 2p region of 47,5A glass surface, before and after soaking for one week in SBF, are reported in figure 11.a and 11.b. After the treatment in SBF, besides the signal of silica at 102.3 eV it is evident the presence of a signal at 103.3 eV, typical of silica gel [15]. By analyzing the peak of O 1s, it was possible to investigate the presence of different oxygen species as a function of the surface treatment. Before any treatment (figure 12.a) the glass shows preferentially a peak at 531.6 eV ascribable to oxygen in silica. Other structural oxides (like Na<sub>2</sub>O, CaO, etc...) are also detectable, before washing, at 530.4 eV. A weak peak at 533 eV is also present due to the presence of few amounts of surface hydroxyls. [16]. After one week in SBF (figure 12.b) the peak at 533 eV grows in intensity, due to the formation of a great amount of a -OH rich species, due to the formation of silanols and silica-gel. At the same time the peak at 530.4 eV (structural oxides) is much higher than before, and this feature is related to the formation of phosphates (early stages of apatite formation) on the glass surface [17].

At the same time, the XPS spectra of C 1s species are modified after soaking in SBF. In detail, the XPS spectra in the C 1s region, detected on the surface of the 47.5 A glass before and after the treatment in SBF, are reported in figure 13.a e 13.b, respectively. In this case, beside the signal at 284.6 due to contaminations, the interesting result is the which can be related to the formation of C-O reach species; in particular the peak at higher energy can be attributed to carbonates which can be involved in the early stages of the hydroxycarbonatoapatite formation [18].

Another interesting aspect is the effect of the treatment in SBF on the molar ratio of some elements (Table III). In particular the Ca/Si, Na/Si, P/Si and K/Si ratios were calculated for as polished samples compared to those soaked in SBF. The treatment in SBF seems to have a strong effect, since both the Na/Si and K/Si ratios decrease on the sample treated in SBF in comparison to the as polished, while the Ca/Si and P/Si ratios increase.

This result can be correlated to the surface reactivity of the glass and to the bioactivity mechanism during the treatments in SBF. The depletion of Na and K is clearly correlated to the ion exchange during the first steps of the bioactivity mechanism, while the enrichment in Ca and P can be considered as the first step of hydroxycarbonatoapatite formation, when calcium and phosphate ions diffuse into the silica gel layer. These

results are in accordance with the XRD pattern of the glass surface after different times of immersion in SBF (figure 6.a).

### 3.4 Biological characterization

Biocompatibility tests performed on 47.5A glass and glass-ceramic demonstrate that the adhesion and proliferation of fibroblast cells line 3T3 onto the materials don't show statistical difference, indicating that the materials are non-toxic for the cells (see figure 14). A good adhesion of cell was noted on glass and glass ceramic with treatment of SBF, while on glass and glass ceramic without SBF, the percentage of cells attached on the materials is lower. A statistical difference was present at day 5 on glass ceramic, glass ceramic with SBF and glass respect to control, but not between them. As demonstrated by the pH measurements and surface characterizations reported in the previous sections, the treatment in SBF gives rise to a fast ion leaching which modifies both the glass surface and the composition of the surrounding solution. This aspect is of great importance in determining the biocompatibility of bioactive glasses and glass-ceramics. After 7 days of treatment in SBF the surface of these materials seems to be more biocompatible, since the ion leaching phenomena, which can negatively affect the cell viability, are already stabilized. Moreover, after this treatment, the glass (or glass-ceramic) surface is covered by a gel-like layer, which is likely to be more hydrophilic than the pristine surface. Such surface can be easily colonized by fibroblasts, that are known to well adhere to hydrophilic surfaces [19].

The results of the proteins adsorption assays are reported in figure 15. This assay gives more precise information about the modalities of interaction of biomaterials *in vivo*.

When biomaterials are implanted *in vivo*, protein adsorption onto the foreign surface occurs immediately after implantation [20-24]. This means that cells arriving at the biomaterial surface probably interact with the adsorbed protein layer rather than directly with the material itself. For this reason, the protein adsorption onto a biomaterial surface plays a key role in the body response to an implanted biomaterial. The first body response to any injury is inflammation, so several studies have been done on the influence of protein adsorption on the inflammatory response. In protein-surface interactions a variety

of governing factors, including bound ions, surface charge, surface roughness, surface elemental composition, surface energy, etc., are determined by the physical state of the material, protein surface and the surrounding environment, and have to be considered in defining the role of the solid-solution interface [25].

In the case of the materials studied in the present work, the high protein adsorption detected on the samples treated in SBF, when compared to the same sample not treated in SBF as well as to control, should be correlated to the presence of the gel-like layer, which appears to promote greater amounts of protein adsorption.

In particular, the attention was focused on IgA and IgG adsorption (figure 16). IgA and IgG are known to be respectively alternative and classical pathway complement activators [26,27]. Their binding to biomaterials might influence complement activation at the material interface [28, 29]. High IgA and IgG binding to both surfaces is index of complement-activating materials.

Proteins adsorption of IgG and IgA, resulted the same for glass and glass ceramic after soaking in SBF, demonstrating that both materials provide a surface capable to properly react against inflammatory processes.

#### **4 Conclusions**

Different sets of glasses and glass-ceramics belonging to the  $\text{SiO}_2\text{-P}_2\text{O}_5\text{-CaO-MgO-K}_2\text{O-Na}_2\text{O}$  system have been prepared and characterized in terms of thermal properties, morphology, composition and phase analysis. Their in vitro bioactivity was investigated and the correlation between the composition and ion leaching was evaluated. The formation of silica-gel and hydroxycarbonatoapatite during soaking in Simulated Body Fluid was investigated by different techniques, revealing few differences between the various glass systems. The surface modifications during soaking in SBF of the most reactive set of samples has been investigated in details. This investigation was useful to understand the different response of virgin glass and glass-ceramic surfaces, compared to pre-treated samples in Simulated Body Fluid, to murine fibroblast 3T3 and the different ability of reacting against inflammatory processes before and after the pre-treatment.

## Acknowledgements

Ministero Italiano della Ricerca e dell'Università (MIUR) (PRIN 2003, "The interface between silica-based materials and biomolecules and/or cell models") is acknowledged for financial support.

## References

1. W. Cao, L.L. Hench, *Ceram. Int.* 22, 493 (1996). doi:[10.1016/0272-8842\(95\)00126-3](https://doi.org/10.1016/0272-8842(95)00126-3)
2. L.L. Hench, *J. Am. Ceram. Soc.* 81(7), 1705 (1998)
3. H. Kim, F. Miyaji, T. Kokubo, *J. Am. Ceram. Soc.* 79(9), 2405 (1995). doi:[10.1111/j.1151-2916.1995.tb08677.x](https://doi.org/10.1111/j.1151-2916.1995.tb08677.x)
4. T. Kokubo, *J. Non-Cryst. Sol.* 120, 138 (1990)
5. T. Kokubo, H. Kushitani, S. Sakka, T. Kitsugi, T. Yamamuro, *J. Biomed. Mater. Res.* 24, 721 (1990). doi:[10.1002/jbm.820240607](https://doi.org/10.1002/jbm.820240607)
6. L. Hench, *J. Am. Ceram. Soc.* 74, 1487 (1991). doi:[10.1111/j.1151-2916.1991.tb07132.x](https://doi.org/10.1111/j.1151-2916.1991.tb07132.x)
7. J.M. Oliveira, R.N. Correia, M.H. Fernandes, *Biomaterials* 16, 849 (1995). doi:[10.1016/0142-9612\(95\)94146-C](https://doi.org/10.1016/0142-9612(95)94146-C)
8. Y. Ebisawa, T. Kokubo, K. Ohura, T. Yamamuro, *J. Mater. Sci. Mater. Med.* 1, 239 (1990). doi:[10.1007/BF00701083](https://doi.org/10.1007/BF00701083)
9. J.M. Oliveira, R.N. Correia, M.H. Fernandes, *Biomaterials* 23, 371 (2002). doi:[10.1016/S0142-9612\(01\)00115-6](https://doi.org/10.1016/S0142-9612(01)00115-6)
10. A.J. Salinas, J. Román, M. Vallet-Regí, J.M. Oliveira, R.N. Correia, M.H. Fernandes, *Biomaterials* 21, 251 (2000). doi: [10.1016/S0142-9612\(99\)00150-7](https://doi.org/10.1016/S0142-9612(99)00150-7)
11. M. Bosetti, M. Cannas, *Biomaterials* 26, 3873 (2005). doi: [10.1016/j.biomaterials.2004.09.059](https://doi.org/10.1016/j.biomaterials.2004.09.059)
12. T. Kokubo, H. Kushitani, S. Sakka, T. Kitsugi, T. Yamamuro, *J. Biomed. Mater. Res.* 24, 721 (1990). doi:[10.1002/jbm.820240607](https://doi.org/10.1002/jbm.820240607)
13. P.W. Mcmillan, *Glass-ceramics* (Academic Press, London, 1979)

14. R.M. Smith, A.E. Martell, R.J. Motekaitis, NIST critical selected stability constants of metal complexes databases, Version 6 (2001)
15. C.D. Wagner, D.E. Passoja, H.A. Six, H.F. Hillery, J.A. Taylor, T.G. Kinisky et al., *J. Vac. Sci. Technol.* 21(4), 933 (1982). doi: [10.1116/1.571870](https://doi.org/10.1116/1.571870)
16. G. Cappelletti, C.L. Bianchi, S. Ardizzone, *Appl. Surf. Sci.* 253, 519 (2006). doi:[10.1016/j.apsusc.2005.12.098](https://doi.org/10.1016/j.apsusc.2005.12.098)
17. H.B. Lu, C.T. Campbell, D.J. Graham, B.D. Ratner, *Anal. Chem.* 72(13), 2886–2894 (2000). doi:[10.1021/ac990812h](https://doi.org/10.1021/ac990812h)
18. Y.W. Gu, K.A. Khor, P. Cheang, *Biomaterials* 25(18), 4127 (2004). doi:[10.1016/j.biomaterials.2003.11.030](https://doi.org/10.1016/j.biomaterials.2003.11.030)
19. N.G. Maroudas, *Nature* 244, 353 (1973). doi:[10.1038/244353a0](https://doi.org/10.1038/244353a0)
20. L. Tang, J.W. Eaton, *Am. J. Clin. Pathol.* 103(4), 466 (1995)
21. J.L. Bohnert, T.A. Horbett, *J. Colloid Interface Sci.* 111, 363 (1986)
22. L. Tang et al., *Biomaterials* 20(15), 1365 (1999). doi: [10.1016/S0142-9612\(99\)00034-4](https://doi.org/10.1016/S0142-9612(99)00034-4)
23. L. Tang, J.W. Eaton, *Mol. Med.* 5(6), 351 (1999)
24. V. Balasubramanian et al., *J. Biomed. Mater. Res.* 44(3), 253 (1999). doi:[10.1002/\(SICI\)1097-4636\(19990305\)44:3<253::AIDJBM3\[3.0.CO;2-K](https://doi.org/10.1002/(SICI)1097-4636(19990305)44:3<253::AIDJBM3[3.0.CO;2-K)
25. J. Israelachvili, *Intermolecular and Surface Forces*, 2nd edn. (Academic Press, London, 1992)
26. K.R. Chintalacharuvu, L.U. Vuong, L.A. Loi, J.W. Larrick, S.L. Morrison, *Clin. Immunol.* 101(1), 21 (2001). doi:[10.1006/clim.2001.5083](https://doi.org/10.1006/clim.2001.5083)
27. S. Hisano, M. Matsushita, T. Fujita, Y. Endo, S. Takebayashi, *Am. J. Kidney Dis.* 38(5), 1082 (2001). doi:[10.1053/ajkd.2001.28611](https://doi.org/10.1053/ajkd.2001.28611)
28. J. Wettero, T. Bengtsson, P. Tengvall, *J. Biomed. Mater. Res.* 51, 742 (2000). doi:[10.1002/1097-4636\(20000915\)51:4<742::AIDJBM24\[3.0.CO;2-D](https://doi.org/10.1002/1097-4636(20000915)51:4<742::AIDJBM24[3.0.CO;2-D)
29. C.S. Rinder, H.M. Rinder, K. Johnson, M. Smith, D.L. Lee, J. Tracey et al., *Circulation* 100, 553 (1999)

## Figures

Fig. 1 XRD pattern of the as done 47.5A glass (a) and glass-ceramic (b)

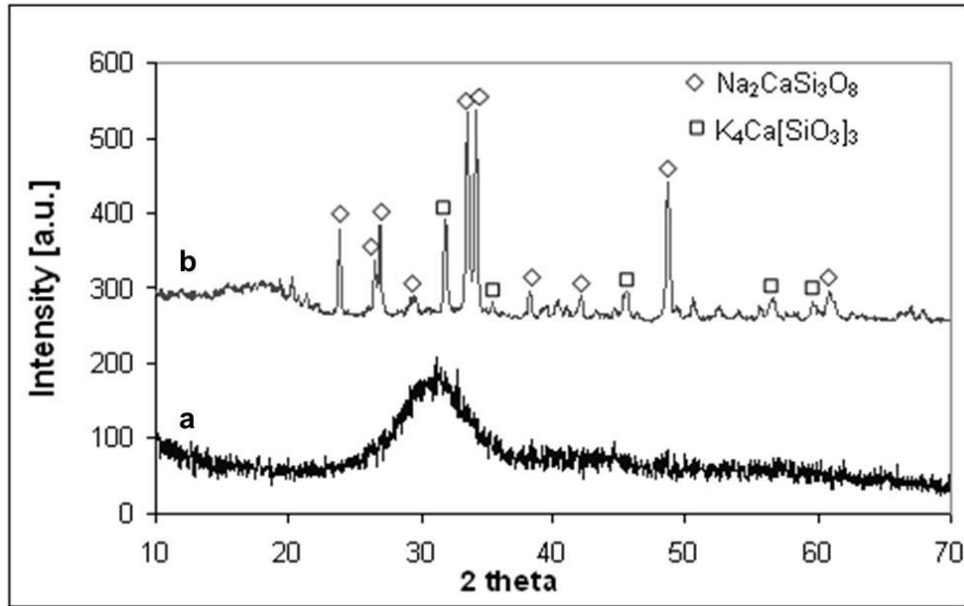


Fig. 2 Morphology of the two crystalline phases detected in the 47.5A glass-ceramic

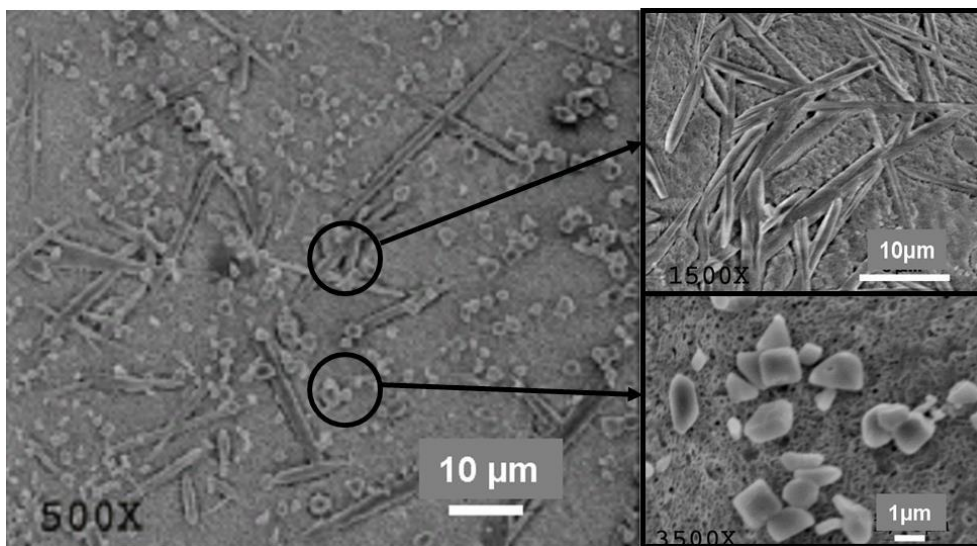


Fig. 3 pH trends of the four glass and glass-ceramic systems soaked in SBF

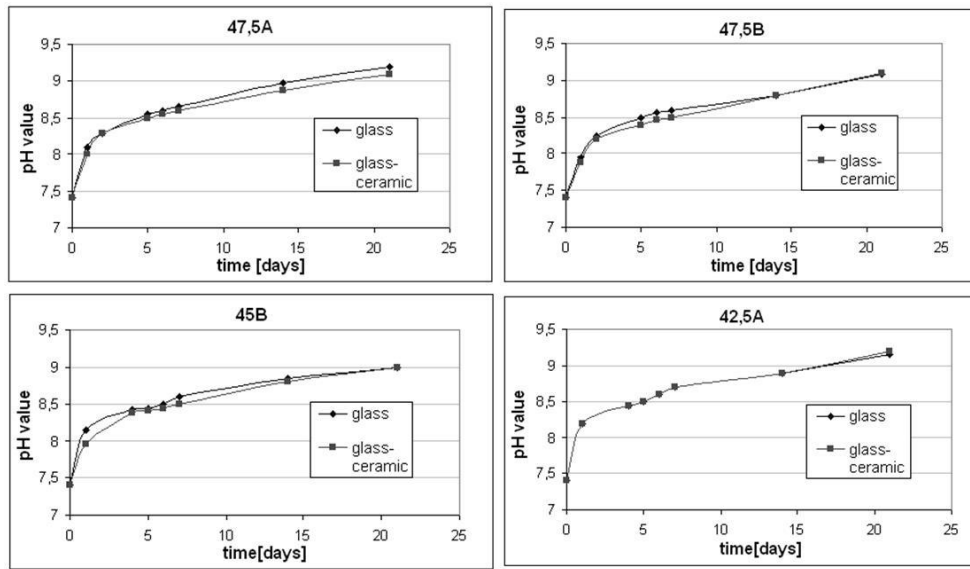


Fig. 4 SEM morphologies of the four bioactive glasses after 21 days of immersion in SBF

(a) 47.5A, (b) 47.5B, (c) 42.5A, (d) 45B

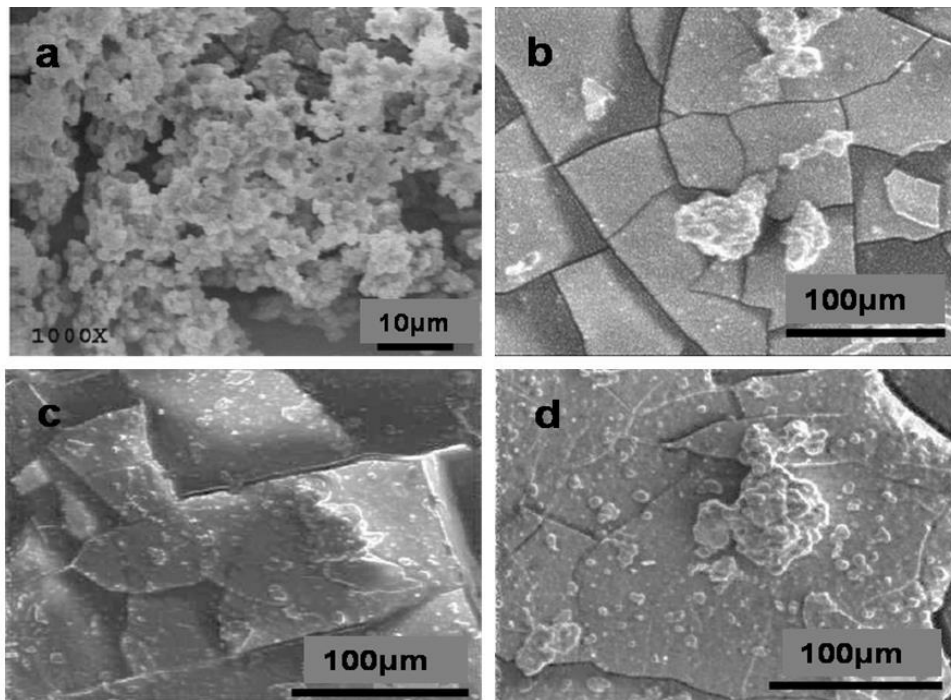


Fig. 5 XRD pattern of of 47.5A, flass, after different times of immersion in SBF, without (a) and with (b) refresh of the solution

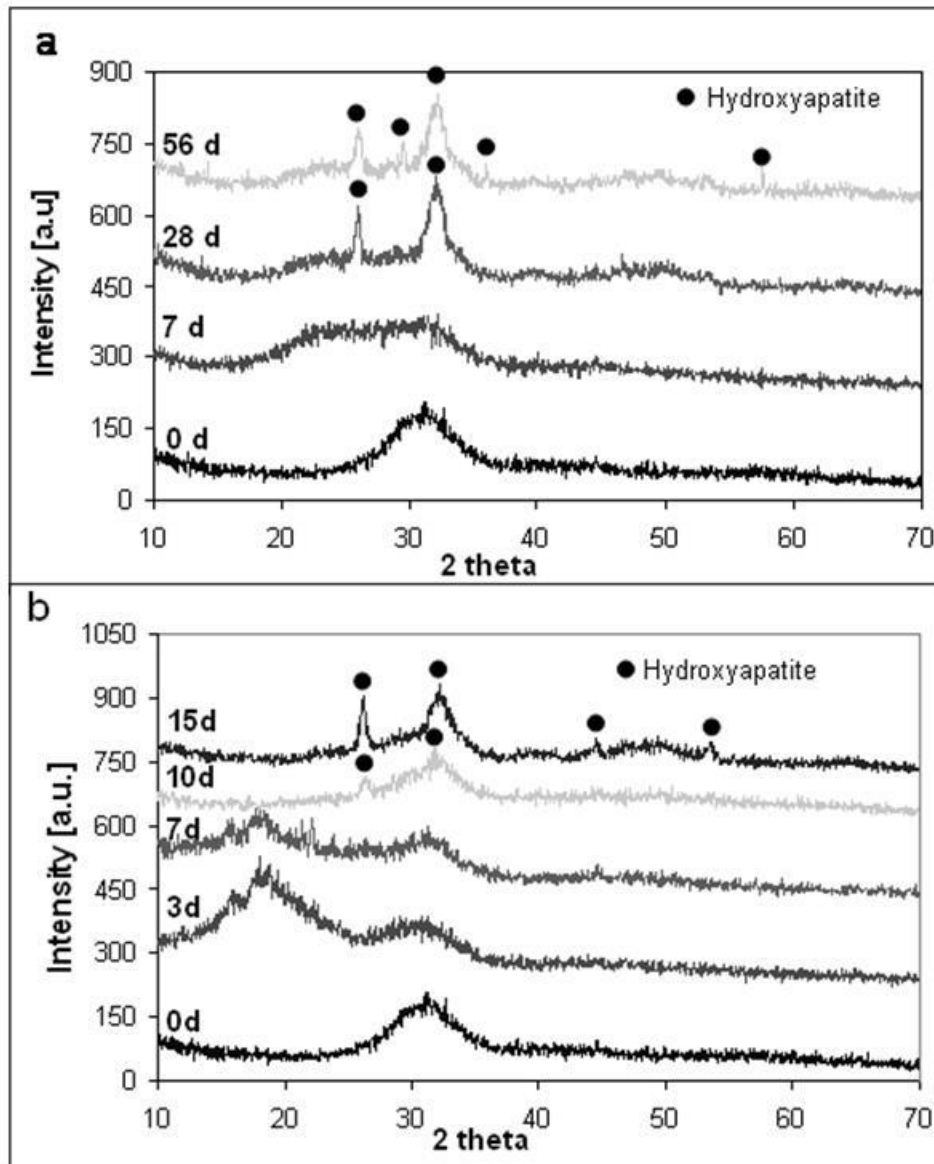


Fig. 6 XRD pattern of 47.5A glass ceramic, after different times of immersion in SBF, without (a) and with (b) refresh of the solution

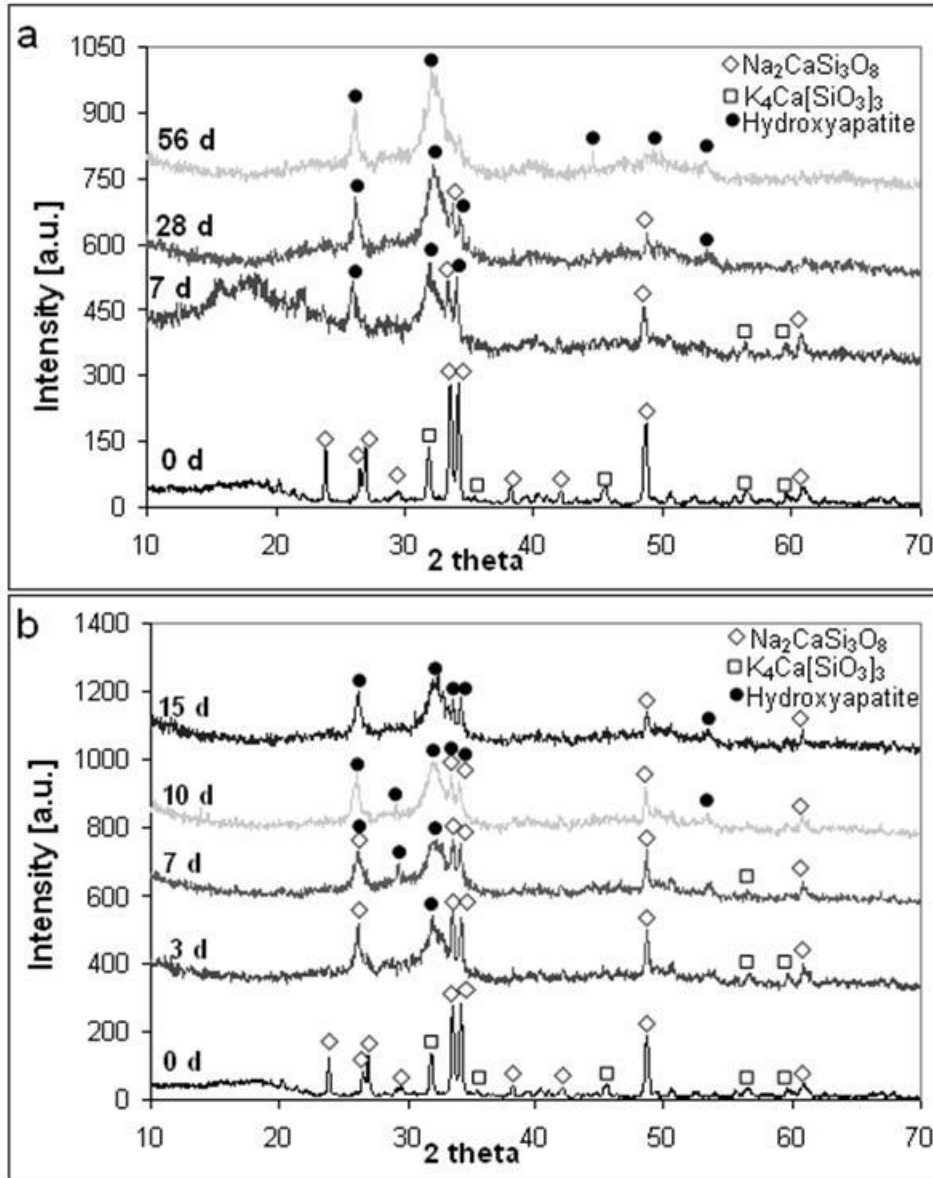


Fig. 7 Morphology (SEM images) and EDS analysis on the glass 47.5A after 7 (a), 28 (b) and 56 (c and d) days of immersion in SBF without refresh of the solution

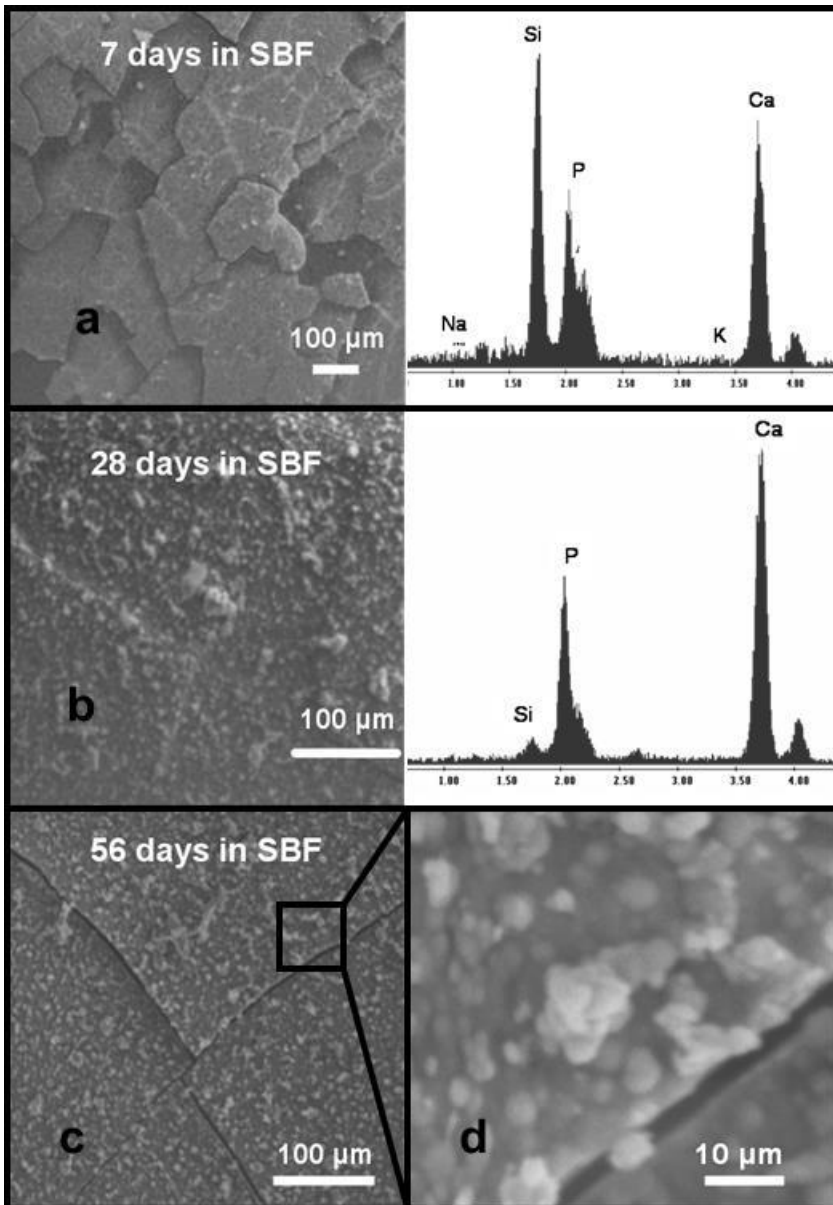


Fig. 8 Morphology (SEM images) and EDS analysis on the glass 47.5A after 3 (a), 7 (b), 10 (c) and 15 (d) days of immersion in SBF with refresh of the solution

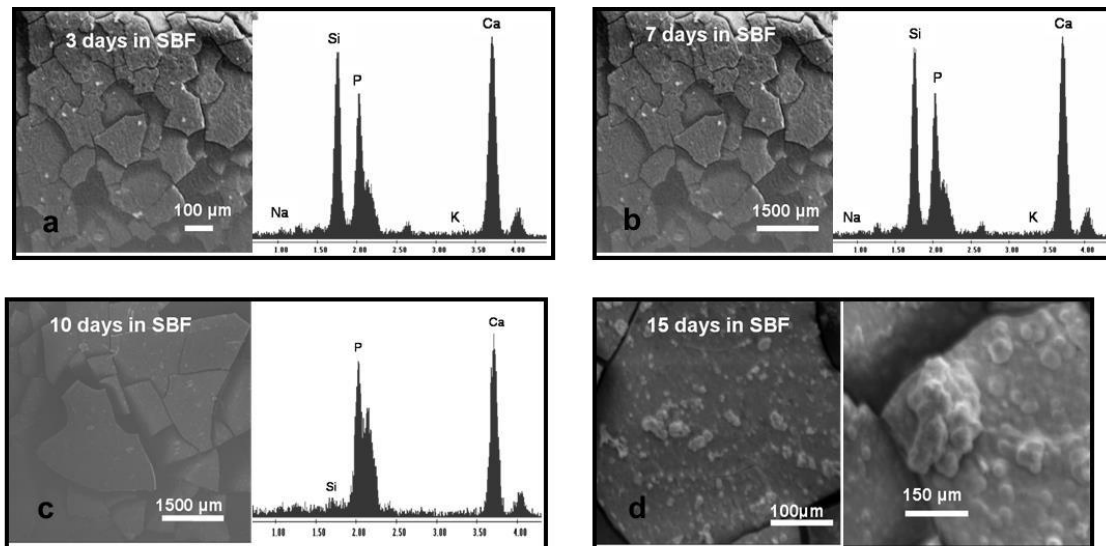


Fig. 9 Morphology (SEM images) and EDS analysis on the glass-ceramic 47.5A after 7 (a), 28 (b) and 56 (c) days of immersion in SBF without refresh of the solution

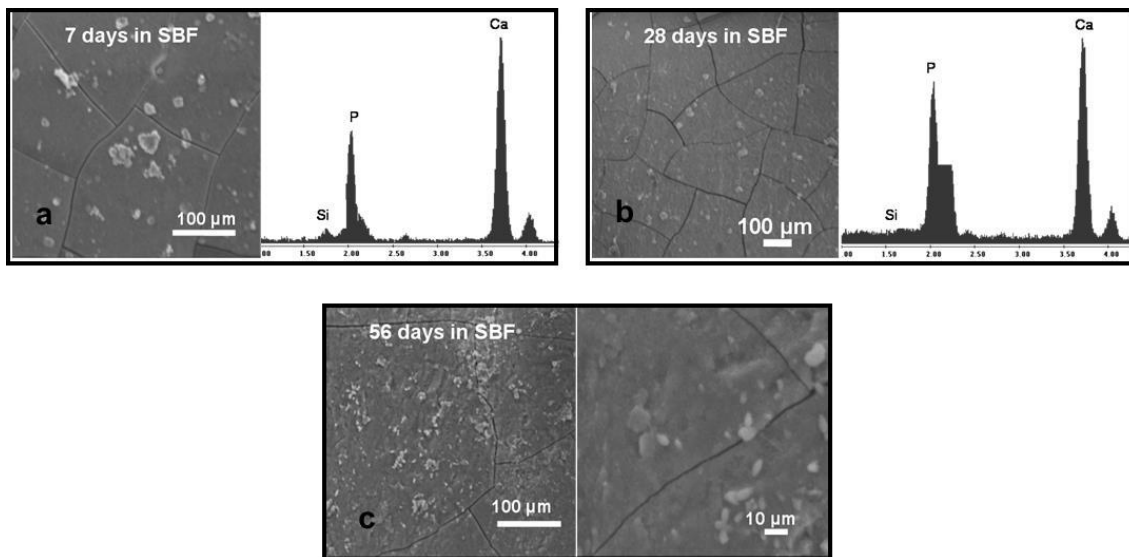


Fig. 10 Morphology (SEM images) and EDS analysis on the glass-ceramic 47.5A after 3 (a), 7 (b), 10 (c) and 15 (d and e) days of immersion in SBF with refresh of the solution

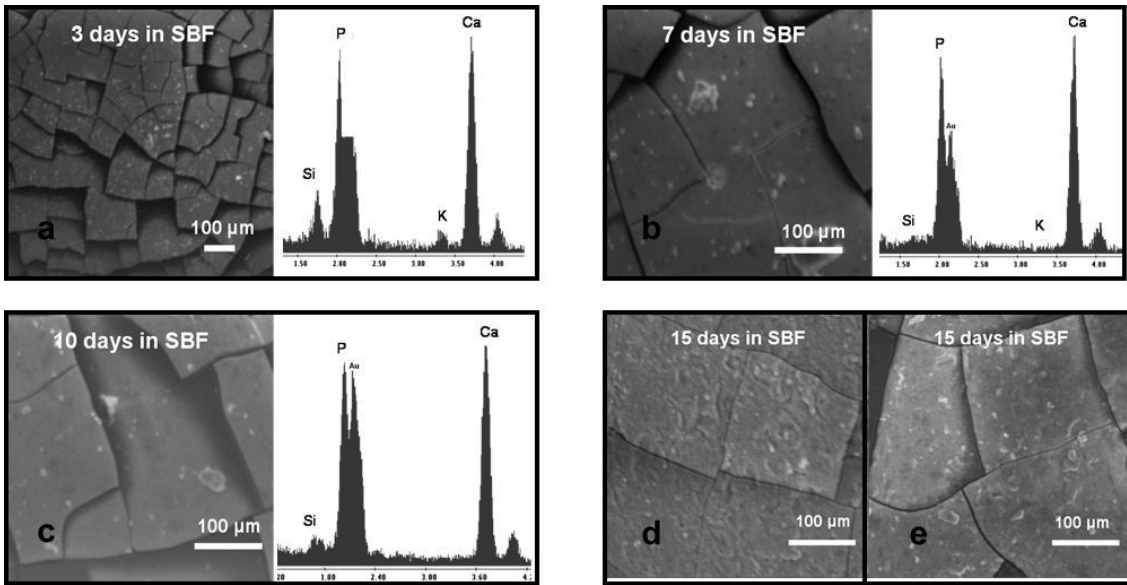


Fig. 11 XPS spectra of the Si 2p region of 47.5A glass surface, before and after soaking for 1 week in SBF

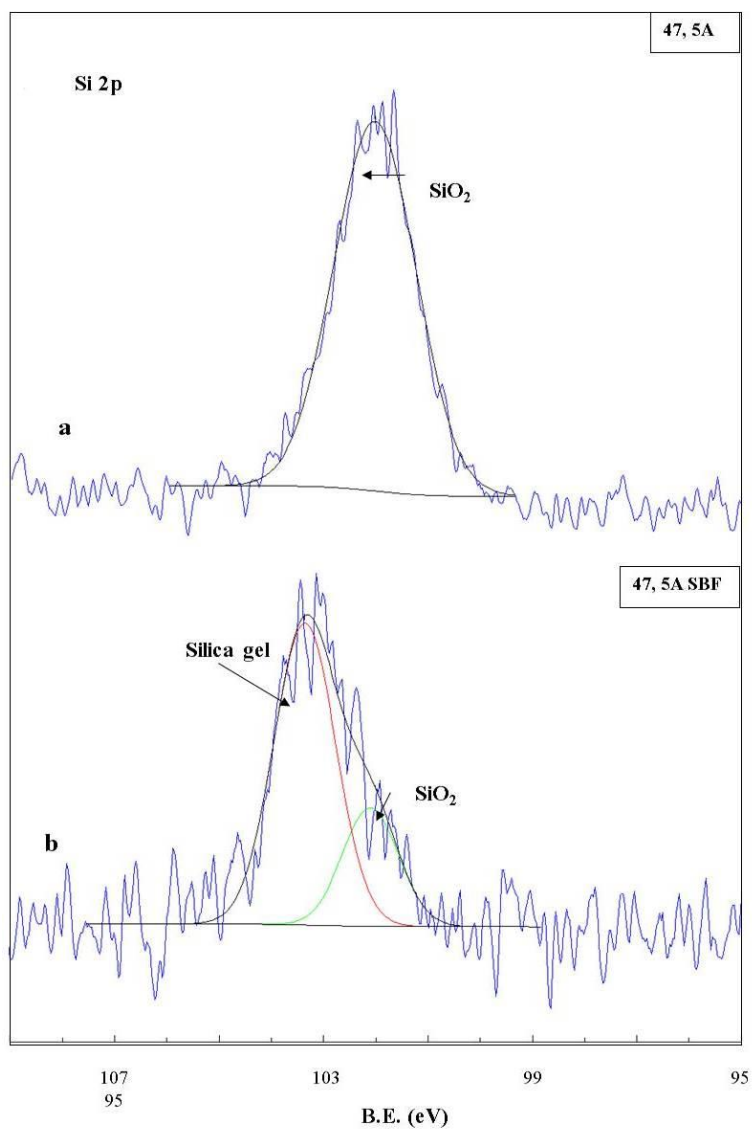


Fig. 12 XPS spectra of the O 1s region of 47.5A glass surface, before and after soaking for 1 week in SBF

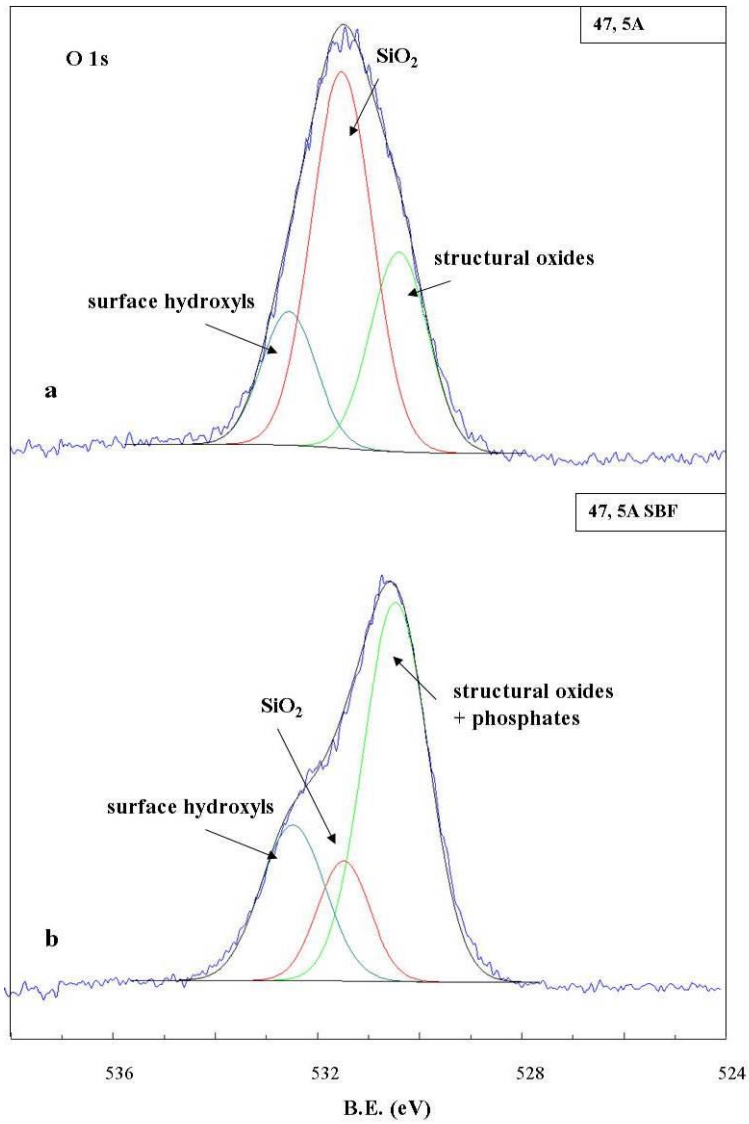


Fig. 13 XPS spectra of the C 1s region of 47.5A glass surface, before and after soaking for 1 week in SBF

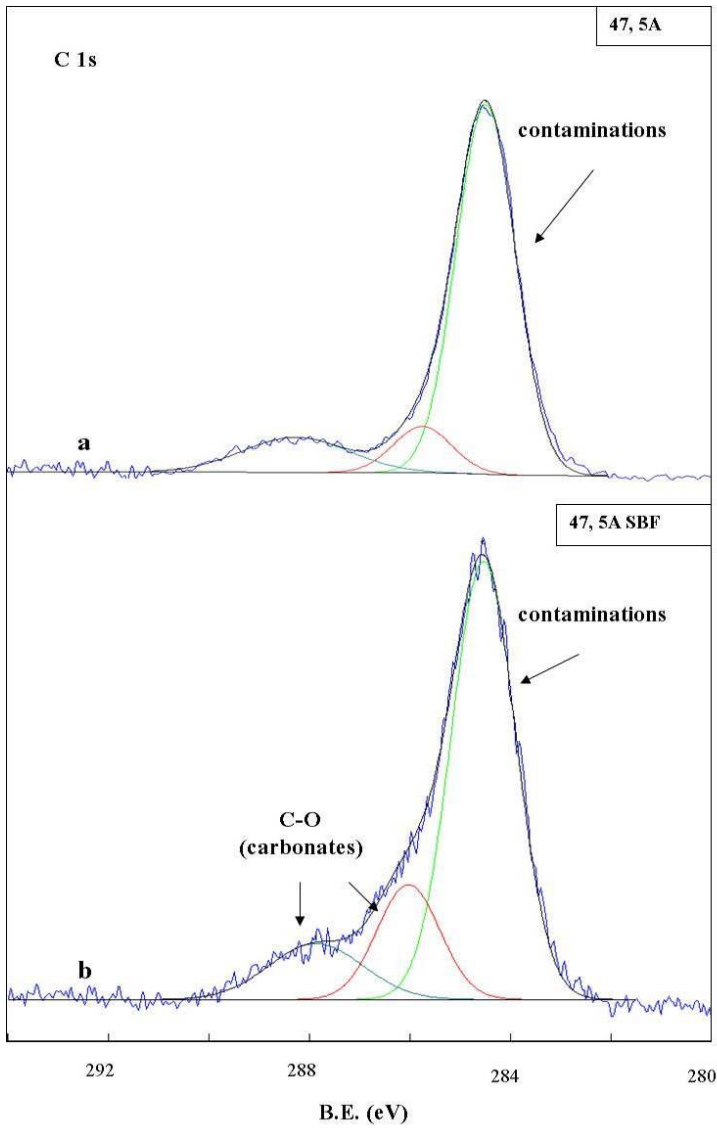


Fig. 14 Adhesion (3 h) and proliferation (5 days) of cell line 3T3 onto glass and glass ceramics, with and without treatment of SBF

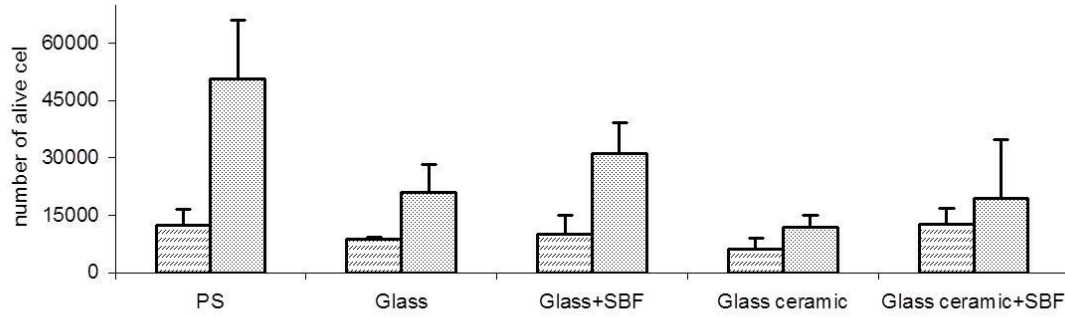


Fig. 15 BCA results for proteins adsorption Optical densities were read at 562 nm against a calibration curve using bovine serum. Results are expressed as micrograms of protein per milliliter

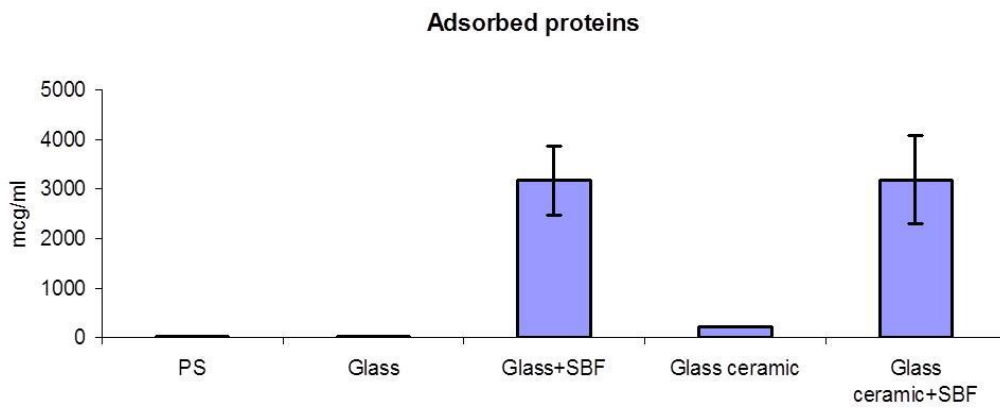
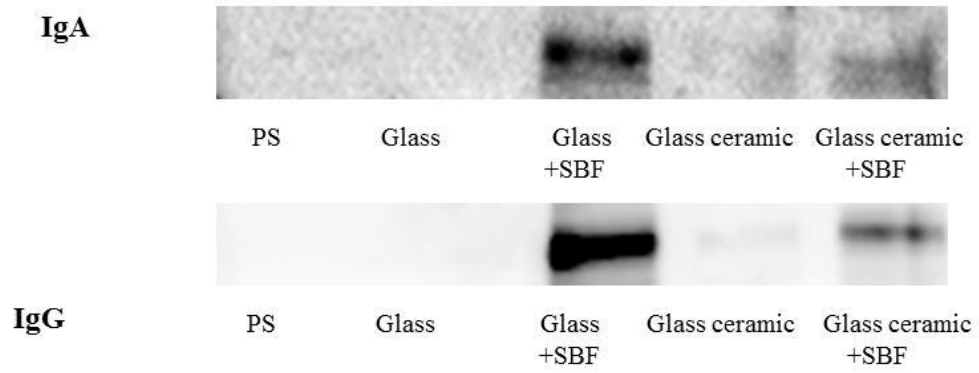


Fig. 16 Immunoblotting of plasma proteins eluted from the materials with rabbit anti-human IgA antiserum, and rabbit anti-human IgG antiserum



## Tables

**Table 1** Compositions (mol%) of the six glasses synthesized in this work

Glass	SiO <sub>2</sub>	P <sub>2</sub> O <sub>5</sub>	CaO	MgO	Na <sub>2</sub> O	K <sub>2</sub> O	SiO <sub>2</sub> +P <sub>2</sub> O <sub>5</sub>
47.5A	47.5	2.5	30	-	10	10	50
47.5B	47.5	2.5	20	10	10	10	50
45A	45	5	25	10	5	10	50
45B	45	5	25	10	10	5	50
42.5A	42.5	2.5	30	15	10	-	45
42.5B	42.5	2.5	30	15	-	10	45

**Table 2** Characteristic temperatures of the four glasses investigated in this work

Glass	T <sub>g</sub> (°C)	T <sub>x1</sub> (°C)	T <sub>x2</sub> (°C)	T <sub>melt 1</sub> (°C)	T <sub>melt 2</sub> (°C)
47.5A	580	800	850	1000	1050
47.5B	540	800	-	1010	-
45B	580	780	880	1000	1250
42.5A	600	830	930	1090	1250

**Table 3** Molar ratios of some elements on the glass as done and after 1 week in SBF

	47.5A	47.5A SBF
Ca/Si	0.3	3.5
Na/Si	0.6	0.3
P/Si	0.1	3.0
K/Si	0.03	0